



Published in final edited form as:

Toxicol Mech Methods. 2012 June ; 22(5): 383–396. doi:10.3109/15376516.2012.673089.

Thiol-redox antioxidants protect against lung vascular endothelial cytoskeletal alterations caused by pulmonary fibrosis inducer, bleomycin: comparison between classical thiol-protectant, *N*-acetyl-L-cysteine, and novel thiol antioxidant, *N,N'*-bis-2-mercaptoethyl isophthalamide

Rishi B. Patel¹, Sainath R. Kotha¹, Lynn A. Sauers¹, Smitha Malireddy¹, Travis O. Gurney¹, Niladri N. Gupta², Terry S. Elton¹, Ulysses J. Magalang¹, Clay B. Marsh¹, Boyd E. Haley², and Narasimham L. Parinandi¹

¹Lipid Signaling, Lipidomics, and Vasculotoxicity Laboratory, Division of Pulmonary, Allergy, Critical Care, and Sleep Medicine, Dorothy M. Davis Heart and Lung Research Institute, College of Medicine, The Ohio State University, Columbus, Ohio, USA

²CTI Science, Inc, Lexington, KY, USA

Abstract

Lung vascular alterations and pulmonary hypertension associated with oxidative stress have been reported to be involved in idiopathic lung fibrosis (ILF). Therefore, here, we hypothesize that the widely used lung fibrosis inducer, bleomycin, would cause cytoskeletal rearrangement through thiol-redox alterations in the cultured lung vascular endothelial cell (EC) monolayers. We exposed the monolayers of primary bovine pulmonary artery ECs to bleomycin (10 µg) and studied the cytotoxicity, cytoskeletal rearrangements, and the macromolecule (fluorescein isothiocyanate-dextran, 70,000 mol. wt.) paracellular transport in the absence and presence of two thiol-redox protectants, the classic water-soluble *N*-acetyl-L-cysteine (NAC) and the novel hydrophobic *N,N'*-bis-2-mercaptoethyl isophthalamide (NBMI). Our results revealed that bleomycin induced cytotoxicity (lactate dehydrogenase leak), morphological alterations (rounding of cells and filipodia formation), and cytoskeletal rearrangement (actin stress fiber formation and alterations of tight junction proteins, ZO-1 and occludin) in a dose-dependent fashion. Furthermore, our study demonstrated the formation of reactive oxygen species, loss of thiols (glutathione, GSH), EC barrier dysfunction (decrease of transendothelial electrical resistance), and enhanced paracellular transport (leak) of macromolecules. The observed bleomycin-induced EC alterations were attenuated by both NAC and NBMI, revealing that the novel hydrophobic thiol-protectant, NBMI, was more effective at µM concentrations as compared to the water-soluble NAC that was effective at mM concentrations in offering protection against the bleomycin-induced EC alterations. Overall, the results of the current study suggested the central role of thiol-redox in vascular EC dysfunction associated with ILF.

© 2012 Informa Healthcare USA, Inc.

Address for Correspondence: Narasimham L. Parinandi, Ph.D., Division of Pulmonary, Allergy, Critical Care, and Sleep Medicine, Dorothy M. Davis Heart and Lung Research Institute, Room # 611-A, 473 West 12th Avenue, College of Medicine, The Ohio State University, Columbus, OH 43210-1252, USA. Tel: (614) 292-8577; Fax: (614) 293-4799. Narasimham.Parinandi@osumc.edu.

Declaration of interest

Overall, there are no conflicts of interest.

Keywords

Cytoskeletal rearrangement; endothelial barrier function; interstitial pulmonary fibrosis; lung vascular endothelial cell; oxidative stress; thiol-redox

Introduction

Idiopathic pulmonary fibrosis (IPF) is a degenerative, chronic, and progressive fibrosing lung disorder of the tissue that lines and separates the alveoli with unknown etiology (Kinnula et al. 2005). The prevalence of IPF in the US is estimated in the range of 35,000 to 55,000 cases as recorded in 2005 (Zisman et al. 2005). Extended exposure to environmental and occupational agents including metal, wood, and stone dusts has been associated with tissue damage that leads to IPF among the idiopathic lung diseases (Taskar and Coultas, 2008; Wilson and Wynn, 2009). In IPF, the tissue that lines and separates the alveoli becomes scarred due to lung damage. This scarring causes the tissue to become inelastic and hard. The buildup of scar tissue causes difficulties in breathing and results in respiratory failure. Interstitial lung diseases (ILD) including sarcoidosis, IPF, and pulmonary Langerhans cell histiocytosis have been shown to be associated with pulmonary hypertension (PH) (Ryu et al. 2007; Cordier, 2008). Lung parenchymal and vascular remodeling indicates the high prevalence (30–40%) of PH among the ILD patients (Behr and Ryu, 2008). Although both the lung epithelium and endothelium have been shown to be critical cellular players in IPF, microvascular injury has been shown as an initial event in the lungs during IPF (Calabrese et al. 2005). The vascular endothelium is crucial as the selective barrier against circulating macromolecules and leukocytes between the blood and interstitium (Everett et al. 2006). In addition, microvascular injury has been emphasized as an important event in the evolution of IPF (Magro et al. 2003). Therefore, the lung microvasculature, more so the lung microvascular endothelium, is apparently an important target in the lung fibrotic events. Studies with experimental models have revealed the role of oxidative stress and antioxidant imbalance in the initiation and progression of IPF, and accordingly redox modulatory therapy has been proposed for the treatment of the disease (Kinnula et al., 2005, 2008). As the lung microvasculature and vascular endothelium are critical regions in IPF, oxidative stress and redox alterations appear to drive the initiation and progression of IPF; it is compelling to rationalize that oxidant-mediated lung microvascular endothelial dysfunction plays a role in the initiation and propagation of IPF.

Vascular endothelial cells (ECs), the inner monolayer lining of blood vessels which form the barrier, are susceptible to oxidative stress that leads to vascular EC disruption and vascular leak. Oxidative stress also leads to the redox perturbation in the vascular ECs such as alterations in the soluble thiols (glutathione, GSH) and protein thiols (Parinandi et al. 1999). Also, earlier we have reported that the bleomycin-induced phospholipase D activation and associated cytotoxicity in lung microvascular ECs is regulated by thiol-redox (Patel et al. 2011). However, the thiol-redox-mediated modulation of the bleomycin-induced cytoskeletal alterations and barrier dysfunction in lung ECs have not been documented. Therefore, here, it is envisioned that oxidative stress induced by bleomycin would cause an imbalance in the thiol-redox of the lung vascular ECs so that the cytoskeletal components, including the actin-cytoskeleton and tight junction proteins, would be altered resulting in the lung vasculature dysfunction. In order to counteract the bleomycin-induced and oxidant-mediated cellular thiol-redox alterations, an effective pharmacological compound with antioxidant and thiol-redox protective properties is needed. As opposed to the most widely used water-soluble, thiol-protectants including *N*-acetyl-L-cysteine (NAC), a hydrophobic and lipid-soluble thiol-protectant would be effective in protecting against the oxidant-induced cellular thiol-redox perturbations in the hydrophobic membrane microenvironments

as well. A novel lipid-soluble hydrophobic compound, *N,N'*-bis-2-mercaptoethyl isophthalamide (NBMI), with both heavy metal-chelating and thiol-redox-protecting properties has been synthesized (Matlock et al. 2001) (Figure 1). NBMI appears to possess the unique features of lipid solubility, membrane lodging, and thiol-redox protection in cells. Hence, in the current study, we used NBMI along with NAC to investigate the role of thiol-redox in the bleomycin-induced and oxidant-mediated cytoskeletal alterations and barrier dysfunction in the bovine pulmonary artery ECs in culture (Figure 1). For the first time, our results revealed that the pulmonary fibrosis inducer, bleomycin, caused endothelial barrier dysfunction, permeability increase, and cytoskeletal alterations through oxidant-mediated thiol-redox alterations, which were protected by the widely used water-soluble thiol-protectant, NAC, and the novel lipid-soluble thiol-protectant, NBMI, with the latter compound being effective at μM concentration.

Materials and methods

Materials

Bovine pulmonary artery endothelial cells (BPAECs; passage 4) were purchased from VEC Technologies (NY). Phosphate-buffered saline (PBS) was obtained from Biofluids Inc. (Rockville, MD). Minimal essential medium (MEM), nonessential amino acids, trypsin, fetal bovine serum (FBS), penicillin/streptomycin, Dulbecco's modified eagle medium (DMEM) phosphate-free modified medium, tissue culture reagents, fluorescein isothiocyanate-dextran (FITC-dextran), NAC, and all other analytical reagents of highest purity were purchased from Sigma Chemical Co. (St. Louis, MO). EC growth factor was obtained from Upstate Biotechnology (Lake Placid, NY). Bleomycin was obtained from Teva Parenteral Medicines (Irvine, CA). The electrical cell-substrate impedance sensing (ECIS) electrode arrays were obtained from Applied Biophysics (Troy, NY). Anti-mouse AlexaFluor 488-conjugated antibody, 4',6-diamidino-2-phenylindole dihydrochloride (DAPI), 6-carboxy-2',7'-dichlorodihydroxyfluorescein diacetate dicarboxy methyl ester (DCFDA), and rhodamine-phalloidin were purchased from Molecular Probes Invitrogen Co. (Carlsbad, CA). Mouse anti-ZO-1 and occludin antibody were obtained from Zymed Laboratories (San Francisco, CA). Paraformaldehyde was purchased from Electron Microscopy Sciences (Fort Washington, PA). Polyethoxylene sorbitan monolaurate (Tween-20) was purchased from Bio-Rad Laboratories (Hercules, CA). Horseradish peroxidase (HRP)-conjugated anti-mouse secondary antibody and the enhanced chemiluminescence (ECL) kit for the detection of proteins by Western blotting were obtained from Amersham (Arlington Heights, IL). GSH assay kit (GSH-Glo) was obtained from Promega Corporation (Madison, WI).

NBMI synthesis

NBMI was synthesized using a modification of the method of Matlock et al. (2003) at the University of Kentucky by Gupta under the supervision of Haley. Three grams of 2-aminoethylthiol hydrochloride was dissolved in 25 ml of chloroform and 3.7 ml of triethylamine and placed in an ice bath with stirring. A total of 2.68 g of isophthaloyl chloride was dissolved in 25 ml of chloroform and slowly added to the solution containing 2-aminoethylthiol and allowed to stir for 2 h on ice. A precipitation of the NBMI was induced by adding about 100 ml of 0.1 N HCl slowly to the stirring mixture. The resulting precipitate was collected by filtration and washed two times with a water:chloroform (50/50) mixture and then two times with 0.1 N HCl and three times with distilled water. The resulting white powder was dried under vacuum and yielded the product NBMI in 70% yield. Gram amounts of this powder were dissolved in pure ethanol and recrystallized twice resulting in the final product. NBMI purity was determined by LC-MS/MS. Column was a Waters X-Bridge C-18 (150 \times 3.0 mm, 5 μm particle size). The mobile phase consisted of (A) aqueous with 0.1% formic acid and (B) methanol with 0.1% formic acid. A gradient

system was used, and the total run time was 30 min. The elution conditions expressed as % of B is as follows: 0–30 s 10% B, 30 s–10 min 10–90% B, 10–19 min 90% B, 19–20 min 90–10% B, and 20–30 min 10% B. Injection volume was 10 μ l. Flow rate was 250 μ l/min and the retention time for NBMI was 9.81 min. Analysis was done on a Varian LC 1200 L Triple Quadrupole MS, using a positive electro-spray ionization source. The pumps were chemicals used in the LC-MS/MS analysis and were purchased from Sigma-Aldrich (St Louis, MO).

Cell culture

BPAECs were grown to confluence in MEM supplemented with 10% (vol/vol) FBS, 100 units/ml penicillin and streptomycin, 5 μ g/ml EC growth factor and 1% (vol/vol) nonessential amino acids at 37°C under a humidified atmosphere of 95% air–5% CO₂ as described earlier (Steinhour et al. 2008). BPAECs, from passages 7 to 15, were used in the experiments. ECs cultured in 35-mm or 60-mm sterile dishes or T-75 cm sterile flasks to ~95% confluence under a humidified atmosphere of 95% air–5% CO₂ at 37°C were used for treatments with bleomycin and desired pharmacological agents. MEM containing bleomycin and other pharmacological agents were carefully adjusted to pH 7.4 for cellular treatments.

Preparation of cell treatment solutions containing pharmacological agents

Stock solutions of the hydrophobic pharmacological agent, NBMI, were freshly prepared in DMSO and diluted in MEM for the treatment of cells. The final DMSO concentration in the cell treatment medium was 0.1% (vol/vol), which did not appear to affect the observed responses in cells. All other solutions of water-soluble pharmacological compounds were freshly prepared in MEM for treatment of cells.

Reactive oxygen species measurement by DCF fluorescence

DCFDA is a lipid-soluble probe that becomes fluorescent when oxidized by multiple forms of reactive oxygen species (ROS). Once DCFDA is taken up by the cell, the intracellular esterases cleave the acetate group of DCFDA and convert it into DCFH₂, which will not be transported out of the cell. Thus, the newly formed DCFH₂ will react with ROS to form fluorescent DCF, which serves as an index of ROS formation. Formation of ROS in BPAECs in 35-mm dishes (5×10^5 cells/dish) was determined by measuring DCF fluorescence in cells preloaded with DCFDA (10 μ M) for 30 min in complete MEM at 37°C under a humidified atmosphere of 95% air–5% CO₂ prior to exposure to bleomycin for 1 h according to our previously published methods (Parinandi et al. 2001; Hagele et al. 2007). At the end of exposure to bleomycin, the cells were detached with a teflon cell scraper, transferred into microcentrifuge tubes, and centrifuged at $8000 \times g$ for 10 min at 4°C. The supernatant was aspirated and the cell pellet was washed twice with ice-cold PBS. Cell lysates were prepared by sonicating the pellets with a probe sonicator at a setting of 2 for 15 s in 500 μ L of ice-cold PBS. Fluorescence of the oxidized DCFDA in cell lysates, as an index of formation of ROS, was measured on a Bio-Tex ELx808 fluorescent plate reader set at 490 nm excitation and 530 nm emission using appropriate blanks. The protein content of the cell lysates was measured and the extent of ROS formation was expressed as arbitrary fluorescence units per mg protein.

GSH determination

Intracellular soluble thiol (GSH) levels were determined using the GSH-Glo GSH assay kit as described earlier (Patel et al. 2011). BPAECs grown up to 90% confluence in 96-well plates were treated with MEM alone or MEM containing bleomycin (10 μ g) or MEM containing selected pharmacological agents and bleomycin for 12 h under a humidified atmosphere of 95% air–5% CO₂ at 37°C. Following incubation, intracellular GSH levels

were determined according to the manufacturer's recommendations and normalized to 10^6 cells (Promega Corp. Madison, WI).

Cellular total thiol determination

Total cellular thiol content was measured by the 5,5'-dithiobis (2-nitrobenzoic acid) (DTNB)-complexed spectrophotometric assay according to our previously published method (Hagele et al. 2007). BPAECs grown up to 90% confluence in 100 mm dishes were treated with MEM alone or MEM containing bleomycin (10 μ g) or MEM containing selected pharmacological agents and bleomycin for 12 h under a humidified atmosphere of 95% air–5% CO₂ at 37°C. At the end of exposure to bleomycin, cells were detached with a teflon cell scraper, transferred into microcentrifuge tubes, and centrifuged at $8000 \times g$ for 10 min at 4°C. The supernatant was aspirated and the cell pellets were lysed using 10% Triton X-100. The cell lysates were treated with DTNB, and then the absorbance was determined at 412 nm on a Bio-Tex ELx808 fluorescent plate reader. Total thiol values were obtained from a standard curve prepared with reduced GSH and normalized to 10^6 cells.

Immunofluorescence microscopy of tight junction proteins

BPAECs cultured on sterile coverslips (Harvard Apparatus, 22 mm²) in 35-mm sterile dishes at a density of 10^4 cells/dish were treated with MEM alone or MEM containing desired concentrations of bleomycin or MEM containing selected pharmacological agents and desired concentration of bleomycin for 4 h under a humidified atmosphere of 95% air–5% CO₂ at 37°C. At the end of the incubation period, cells cultured on coverslips were washed with PBS, fixed with 3.7% of paraformaldehyde for 10 min, permeabilized with 0.25% Triton X-100 in Tris-buffered saline Tween-20 (TBST) containing 0.01% Tween-20 for 5 min, blocked for 30 min with 1% BSA in 0.01% TBST, and then incubated for 12 h at room temperature with mouse primary anti-occludin and anti-ZO-1 antibodies at a dilution of 1:200 (vol/vol) for the visualization of tight junction protein localized on the cellular membrane. Following the treatment of cells with the primary antibody, the cells were incubated with secondary anti-mouse AlexaFluor 488-conjugated antibody (1:100 dilution, vol/vol) for 1 h at room temperature. The coverslips with cells were then mounted on a glass slide with the antifade mounting medium, Fluoromount-G, and viewed with Zeiss Confocal microscope at 63 \times magnification. The pictures were captured digitally, and the fluorescence intensity was quantified using the Scion Image software (Scion-image.software.informer.com).

Fluorescence microscopy of actin stress fibers

Formation of actin stress fibers, as an index of endothelial cytoskeletal reorganization, was examined by fluorescence microscopy according to our previously published method (Sliman et al., 2010). BPAECs cultured on sterile coverslips (Harvard Apparatus, 22 mm²) in 35-mm sterile dishes at a density of 10^4 cells/dish were treated with MEM alone or MEM containing desired concentrations of bleomycin or MEM containing selected pharmacological agents and desired concentration of bleomycin for 4 h under a humidified atmosphere of 95% air–5% CO₂ at 37°C. At the end of the incubation period, cells cultured on coverslips were washed with $1 \times$ PBS, fixed with 3.7% of paraformaldehyde for 10 min, permeabilized with 0.25% Triton X-100 in TBST containing 0.01% Tween-20 for 5 min, and blocked for 30 min with 1% BSA in 0.01% TBST. Actin stress fibers were visualized by staining the cells with rhodamine-phalloidin (1:50 dilution) in 1% BSA in TBST for 1 h. The cells were then washed four times with PBS, stained with 1% DAPI in PBS for 5 min, washed four times with PBS, mounted, and examined under Zeiss LSM 510 Confocal/Multiphoton Microscope at 543 nm excitation and 565 nm emission under 63 \times

magnification. The images were captured digitally. The extent of the fluorescence intensity was measured using the Scion Image software.

Morphology assay of cytotoxicity

Morphological alterations in BPAECs cultured in 35-mm dishes up to 70% confluence, following their exposure to bleomycin and other pharmacological treatments for 12 h, were examined as an index of cytotoxicity according to our previously established method (Mazerik et al. 2007). Images of cell morphology were digitally captured with the Olympus microscope at 20× magnification.

Measurement of transendothelial cell electrical resistance

The transendothelial cell electrical resistance (TER) was measured according to our previously published method (Sliman et al. 2010). BPAECs were cultured up to 90% confluence in complete MEM on gold electrodes (Applied Biophysics Inc., Troy, NY) under a humidified atmosphere of 95% air–5% CO₂ at 37°C. The EC monolayers were then treated with MEM alone or MEM containing the desired concentrations of the pharmacological agents for 2 h. TER of the monolayers was continuously measured on ECIS (Applied Biophysics Inc., Troy, NY) following the treatment of cells with MEM containing bleomycin (10 µg) under a humidified atmosphere of 95% air–5% CO₂ at 37°C.

Measurement of paracellular endothelial permeability

BPAECs were grown to 80% confluence in 12-well Corning 3.0 µm pore-size culture inserts (Lowell, MA). The EC monolayers were treated with MEM alone or MEM containing the desired concentrations of pharmacological agents for 2 h and then with MEM containing selected pharmacological agents and bleomycin (10 µg) for 12 h under a humidified atmosphere of 95% air–5% CO₂ at 37°C. Following treatments, FITC-dextran (30 kDa) dissolved in phenol-free MEM was placed on the apical side of the monolayer, in the insert, and the cells were then incubated for 1 h under a humidified atmosphere of 95% air–5% CO₂ at 37°C. The fluorescence of the FITC-dextran that leaked through the paracellular gaps of the EC monolayer was measured on a Bio-Tex ELx808 fluorescent plate reader set at 480 nm excitation and 540 nm emission, using appropriate blanks. The extent of FITC-dextran found in the basal side of the EC monolayer was expressed as arbitrary fluorescence units.

Protein determination

The amount of protein in the cells and cell lysates was determined by the BCA protein assay (Thermo Scientific, Rockford, IL).

SDS-polyacrylamide gel electrophoresis and Western blotting

Preparation of cell lysates and Western blotting were carried out according to our previously published methods (Varadharaj et al. 2006). Cell lysates containing 40 µg of protein were loaded onto a 10% SDS-polyacrylamide gel electrophoresis (SDS-PAGE) gel and proteins were separated at 90 V for 2.5 h. Proteins resolved on gels were electrotransferred onto the polyvinylidene difluoride (PVDF) membranes at 200 mA for 2 h at 4°C. PVDF membranes with proteins were then washed with 0.05% Tween-20 in Tris-buffered saline (TBST) following which they were blocked with TBST containing 5% milk for 1 h and then incubated with the primary antibody (1:1000 dilution) at 4°C overnight in TBST containing 5% BSA. Membranes were then treated with HRP-conjugated anti-mouse IgG (1:2000 dilution) in TBST containing 5% milk at room temperature for 1 h followed by washing for three times with TBST. The immunoblots were then developed with the ECL reagents

according to the manufacturer's recommendations. Images on films were scanned and quantified using the Scion Image software.

Lactate dehydrogenase release assay of cytotoxicity

Cytotoxicity in ECs was determined by assaying the extent of release of lactate dehydrogenase (LDH) from cells according to our previously published method (Mazerik et al. 2007). ECs cultured up to 90% confluence in 17.5-mm dishes were treated with MEM alone or MEM containing NAC (50 μ M) or NBMI (50 μ M) for 2 h and then with MEM alone or MEM containing NAC or NBMI with bleomycin (10 μ g) for 6 h under a humidified atmosphere of 95% air–5% CO₂ at 37°C. At the end of treatment, the medium was collected and LDH released into the medium was determined spectrophotometrically according to the manufacturer's recommendations (Sigma Chemical Co., St. Louis, MO).

Statistical analysis

All experiments were done in triplicate. Data were expressed as mean \pm standard deviation (SD). Statistical analysis was carried out by ANOVA using SigmaStat (Jandel). The level of statistical significance was taken as $p < 0.05$.

Results

NAC and NBMI protect against bleomycin-induced morphological alterations in ECs

Altered cell morphology serves as a suitable index to assess cytotoxicity. Accordingly, earlier we have reported that bleomycin causes cell morphology alterations (Patel et al. 2011). Therefore, here, we investigated whether the thiol-protectants, NAC and NBMI, would offer protection against the bleomycin-induced cell morphology alterations. BPAECs were pre-treated for 1 h with MEM alone or MEM containing the chosen antioxidant (5 mM of NAC and 50 μ M of NBMI) and then treated with bleomycin (10 μ g) for 12 h, and then subjected to cell morphology examination by light microscopy. Bleomycin caused significant morphological alterations in the EC morphology with the rounding of the cells and filipodia formation (Figure 2). Both NAC and NBMI markedly attenuated the bleomycin-induced cell morphological alterations at 12 h, suggesting the role of thiol-redox in the bleomycin-induced cytotoxicity and EC monolayer dysfunction (Figure 2).

NAC and NBMI protect against bleomycin-induced cytotoxicity in ECs

As it was shown in this study that bleomycin caused morphological alterations in ECs, here, another measure of cytotoxicity, the release of LDH by the ECs exposed to bleomycin was used and the protective effect of NAC and NBMI on LDH release was investigated. BPAECs were pre-treated for 1 h with MEM alone or MEM containing the chosen thiol-protectant (50 μ M and 5 mM of NAC, and 50 μ M of NBMI) and then treated with bleomycin (10 μ g) for 6 h. Bleomycin caused significant LDH release (1.7-fold increase) as compared with the same in the control untreated cells. The bleomycin-induced LDH release was significantly attenuated by NAC and NBMI (56% and 67% of inhibition by 5 mM NAC and 50 μ M NBMI, respectively; Figure 3). NAC at 50 μ M dose did not appear to offer significant protection against the bleomycin-induced LDH leak. These results indicated that the bleomycin-induced cytotoxicity in ECs, as evidenced by LDH release, was protected by NAC and the novel thiol-protectant, NBMI, wherein mM dose of NAC was required to attenuate the bleomycin-induced LDH release by the ECs as compared to NBMI, which caused significant attenuation of the same at μ M dose.

NAC and NBMI protect against bleomycin-induced ROS generation in ECs

The pharmacological action of bleomycin has been associated with its ability to induce ROS formation (Ghio, 2009). Studies have shown that oxidants induce endothelial barrier dysfunction (Usatyuk et al. 2006; Uchida 2003). However, the role of thiol-redox in the bleomycin-induced ROS generation in ECs has not been shown. Therefore, here, we investigated the ability of the chosen thiol-protectants (NAC and NBMI) to attenuate the bleomycin-induced intracellular ROS formation in BPAECs by determining the DCF fluorescence. Cells were pre-treated for 1 h with MEM alone or MEM containing the chosen thiol-protectant (5 mM of NAC and 50 μ M of NBMI) and then co-treated for 1 h with bleomycin (5, 10, or 100 μ g) and the chosen thiol-protectant. Bleomycin, at 1 h of treatment, significantly induced the ROS formation in BPAECs as compared with that in the control untreated cells (1.3-, 2.8-, and 2.4-fold at 5, 10, and 100 μ g, respectively) (Figure 4A). Furthermore, the classical thiol-protectant, NAC, and the novel thiol-protectant, NBMI, offered effective and significant attenuation of the bleomycin-induced ROS formation in BPAECs (70% and 87% for NAC and NBMI, respectively) (Figure 4B). These results demonstrated that bleomycin induced the intracellular ROS formation in ECs and that the novel lipid-soluble thiol-protectant, NBMI, at a μ M dose offered significant attenuation of the bleomycin-induced ROS formation that was similar to the protection offered by a mM dose of the classical water-soluble thiol-protectant, NAC.

NAC and NBMI protect against bleomycin-induced GSH and total thiol depletion in ECs

Earlier in this study, we showed that bleomycin induced the formation of ROS in ECs and that the thiol-protectants, NAC and NBMI, were effective in attenuating the bleomycin-induced ROS formation. Therefore, here, we hypothesized that bleomycin would cause the depletion of intracellular GSH and the cellular total thiol levels and the thiol-protectants (NAC and NBMI) would attenuate the bleomycin-induced depletion of GSH and total thiols in BPAECs. Cells were pre-treated for 1 h with MEM alone or MEM containing the chosen thiol-protectant (5 mM of NAC and 50 μ M of NBMI) and then co-treated for 12 h with bleomycin (5, 10, or 100 μ g) and the chosen thiol-protectant. Bleomycin, at 12 h of treatment, effectively induced a significant cellular GSH depletion in BPAECs as compared with that in the control untreated cells (108%, 98%, and 2182% of decrease at 5, 10, and 100 μ g, respectively) (Figure 5A). NAC and NBMI offered effective and significant attenuation of the bleomycin-induced GSH depletion in BPAECs (43% and 96% for NAC and NBMI, respectively) (Figure 5B). Bleomycin also induced a significant loss of the total thiol levels in BPAECs at 12 h of treatment (53% loss). Also, NAC and NBMI offered significant attenuation of the bleomycin-induced loss of cellular total thiols (51% and 81% for NAC and NBMI, respectively) (Figure 5C). These results demonstrated that bleomycin induced the loss of intracellular GSH and total thiols in ECs and that the novel lipid-soluble thiol-protectant, NBMI, at a μ M dose offered significant attenuation that was similar to the protection offered by a mM dose of the classical water-soluble thiol-protectant, NAC.

NAC and NBMI protect against bleomycin-induced transendothelial barrier dysfunction

Studies have revealed the role of oxidative stress and antioxidant imbalance in the initiation and progression of IPF (Kinnula et al. 2005). As bleomycin is an oxidant drug, we envisioned that it would cause transendothelial barrier dysfunction. Therefore, here, we studied whether bleomycin would induce transendothelial barrier dysfunction and whether the thiol-protectants, NAC and NBMI, would offer protection against the bleomycin-induced transendothelial dysfunction in BPAECs. The transendothelial barrier integrity was quantified by measuring the TER of the EC monolayer. Cells grown on gold electrodes were pre-treated for 1 h with MEM alone or MEM containing the chosen thiol-protectant (5 mM of NAC and 50 μ M of NBMI) and then treated with bleomycin (5, 10, or 100 μ g). Bleomycin induced a significant decrease in the TER starting at 4 h of treatment (Figure

6A). Additionally, NAC and NBMI offered marked attenuation of the bleomycin-induced transendothelial barrier dysfunction in BPAECs (Figure 6B and 6C). Hence, these results demonstrated that bleomycin induced the transendothelial dysfunction, which was attenuated by the novel lipid-soluble thiol-protectant, NBMI, and the classical water-soluble thiol-protectant, NAC.

NAC and NBMI protect against bleomycin-induced paracellular permeability in EC monolayer

Earlier in this study, bleomycin was shown to induce transendothelial barrier dysfunction (decrease in TER), which was protected by the thiol-protectants NAC and NBMI. Therefore, here, we studied whether bleomycin would cause increased paracellular permeability (an index of transendothelial barrier dysfunction) and whether the thiol-protectants, NAC and NBMI, would offer protection against the bleomycin-induced increase in paracellular permeability of macromolecules in BPAEC monolayer. The paracellular barrier integrity was quantified by measuring the permeability of the FITC-dextran, a 30 kDa macromolecule, through the paracellular gaps of the EC monolayer. Cells grown on filters were pre-treated for 1 h with MEM alone or MEM containing the chosen thiol-protectant (5 mM of NAC and 50 μ M of NBMI) and then treated with bleomycin (10 μ g) for 12 h. Bleomycin induced a significant increase in the permeability of FITC-dextran through the EC monolayer (43% and 66%) (Figure 7A and 7B). NAC offered effective and significant attenuation of the bleomycin-induced FITC-dextran leak in ECs (25% attenuation) (Figure 7A). NBMI also showed remarkable and significant protection against this bleomycin-induced leak (16% attenuation) (Figure 7B). These results demonstrated that bleomycin induced the paracellular barrier dysfunction, which was attenuated by the novel lipid-soluble thiol-protectant, NBMI, and the classical water-soluble thiol-protectant, NAC.

NAC and NBMI protect against bleomycin-induced actin cytoskeletal reorganization in ECs

The regulation of cytoskeleton is important for the cell size, shape, and motility (Bogatcheva and Verin, 2008). The actin cytoskeletal reorganization in ECs under stress is known to contribute to the stress-induced loss of TER and barrier dysfunction in EC monolayers (Chiang et al. 2009). The actin stress fiber formation in ECs during stress is a commonly recognized cytoskeletal response indicating the actin cytoskeletal reorganization (Vandenbroucke et al. 2008). Hence, in this study, we examined whether bleomycin would cause the actin cytoskeletal reorganization (actin fiber formation) and whether the thiol-protectant, NAC and NBMI, would offer protection against such EC response. Cells grown on coverslips were pre-treated for 1 h with MEM alone or MEM containing the chosen thiol-protectant (5 mM of NAC and 50 μ M of NBMI) and then treated with bleomycin (5, 10, 100 μ g) for 4 h. Bleomycin induced the formation of actin stress fibers in BPAECs in a dose-dependent manner at 4 h of treatment (Figure 8A). Furthermore, the treatment of cells with both NAC and NBMI significantly attenuated the bleomycin (10 μ g)-induced actin stress fiber formation in ECs at 4 h of treatment (Figure 8C and 8E). These results revealed that bleomycin induced the actin cytoskeletal reorganization and the thiol-protectants, NAC and NBMI, offered protection against such cytoskeletal response in ECs.

NAC and NBMI protect against bleomycin-induced tight junction protein, ZO-1, alterations in ECs

Tight junctions are crucial for the cell-to-cell adhesion and the maintenance of the tight barrier in the EC monolayer (Fasano, 2000). ZO-1 is a key tight junction protein that contributes to the maintenance of the cellular tight junctions (Xu et al. 2007). Stress is known to alter the EC tight junctions through the ZO-1 proteins (Harhaj and Antonetti, 2004). Therefore, here, we investigated whether bleomycin would alter the ZO-1 protein organization in ECs and whether the thiol-protectants, NAC and NBMI, would attenuate

such alterations. Cells grown on coverslips were pre-treated for 1 h with MEM alone or MEM containing the chosen thiol-protectant (5 mM of NAC and 50 μ M of NBMI) and then treated with bleomycin (5, 10, 100 μ g) for 4 h. Bleomycin induced marked disappearance of the regular localization of ZO-1 around the cell periphery of the ECs in a dose-dependent manner at 4 h of treatment (Figure 9A). Furthermore, the treatment of cells with both NAC and NBMI significantly restored the bleomycin (10 μ g)-induced disturbance of ZO-1 in ECs at 4 h of treatment (Figure 9C and 9E). These results demonstrated that bleomycin induced the disappearance of ZO-1 protein leading to the alteration in the organization of tight junctions of the ECs, which was protected by the thiol-protectants, NAC and NBMI.

NAC and NBMI protect against bleomycin-induced tight junction protein, occludin, alterations in ECs

Earlier in this study, we demonstrated the bleomycin induced the alteration of key tight junction protein, ZO-1, in ECs. These alterations were attenuated by the thiol-protectants, NAC and NBMI. Occludin is another important tight junction protein that contributes to the maintenance of the cellular tight junctions. Thus, we investigated whether bleomycin would also alter the occludin protein organization in ECs and whether the thiol-protectant, NAC and NBMI, would attenuate such alterations. Cells grown on coverslips were pre-treated for 1 h with MEM alone or MEM containing the chosen thiol-protectant (5 mM of NAC and 50 μ M of NBMI) and then treated with bleomycin (5, 10, 100 μ g) for 4 h. Bleomycin induced a marked disappearance of occludins around the cell periphery of the ECs in a dose-dependent manner at 4 h of treatment (Figure 10A). Furthermore, the treatment of cells with both NAC and NBMI significantly restored the bleomycin (10 μ g)-induced disappearance of occludins in ECs at 4 h of treatment (Figure 10C and 10E). These results established that bleomycin also induced the disappearance of occludin protein leading to the alteration in the organization of tight junctions of the ECs, which was protected by the thiol-protectants, NAC and NBMI.

Bleomycin causes loss of tight junction proteins in ECs

Earlier in this study, we showed that bleomycin induced alterations in the organization of endothelial tight junction proteins, ZO-1 and occludins, at 4 h of treatment. Therefore, here, we studied whether bleomycin would induce the loss of these proteins. Cells treated for 4 h with bleomycin (5, 10, or 100 μ g) were harvested and the tight junction proteins were isolated and measured by SDS-PAGE and Western blotting. Bleomycin, at 4 h of treatment, effectively induced a significant loss of ZO-1 in BPAECs as compared with that in the control untreated cells (55%, 61%, and 68% of decrease at 5, 10, and 100 μ g, respectively) (Figure 11A and 11B). Bleomycin also induced a significant loss of occludin in BPAECs as compared with that in the control untreated cells (48%, 53%, and 60% of decrease at 5, 10, and 100 μ g, respectively) (Figure 11A and 11C).

Discussion

The results of the current study revealed that bleomycin at pharmacological doses (μ g) induced the loss of endothelial barrier function, which was attenuated by the thiol-protective antioxidants, NAC and NBMI, suggesting the upstream role of oxidants and altered thiol-redox signaling in the bleomycin-induced barrier dysfunction in BPAECs. This was further confirmed by the enhanced generation of ROS and decrease in thiol levels upon treatment of BPAECs with bleomycin. NAC and NBMI caused significant inhibition of the bleomycin-induced loss of endothelial barrier function and also offered protection against the loss of tight junction proteins of the ECs. The bleomycin-induced cytotoxicity, generation of ROS, and decrease in thiol levels were attenuated by NAC and NBMI. Furthermore, the current study also revealed that the effectiveness of the lipid-soluble thiol-protectant, NBMI, at μ M

concentrations, is comparable to mM concentrations of the water-soluble thiol-protectant, NAC.

Pulmonary fibrosis is a fibrotic disorder where abnormal wound healing causes fibroblasts to proliferate excessively, characterized by excess deposition of extracellular matrix components such as collagen and fibronectin (Gross and Hunninghake, 2001). Bleomycin is an oxidant chemotherapeutic drug that is widely used to induce experimental lung fibrosis in animal models (Jackson, 1985; Tashiro et al. 2008; Fang, 2000). Iron and iron-redox are thought to play a key step in bleomycin-induced ROS production (Burger et al. 1979; Antholine et al. 1981). Bleomycin-induced lung damage has been shown to occur in three stages. First, bleomycin induces the apoptosis and necrosis of the alveolar epithelial cells, followed by an inflammatory stage where there is an influx of neutrophils and lymphocytes to the interstitium of the lung. Then, unregulated repair and remodeling process result in excessive deposition of collagen and fibronectin (Moore and Hogaboam, 2008; Rojas et al. 2005). The overproliferation of the fibroblasts is signaled by an increase in the secretion of cytokines such as the tumor necrosis factor- α and platelet-derived growth factor (Li et al. 2004; Oikonomou et al. 2006). Pro-inflammatory cytokines are produced largely by the leukocytes that infiltrate the lung interstitium during the endothelial barrier dysfunction in the first stage of bleomycin-induced lung damage (Vaillant et al. 1996; Warshamana et al. 2002; Petri and Bixel, 2006).

The proper function of the lung microvascular endothelium is crucial for the separation of the macromolecules of the blood from the lung interstitium. The infiltration and presence of neutrophils and lymphocytes in the interstitium that leads to inflammation, the second stage of the bleomycin-induced lung damage, has been well studied (Iyer et al. 2009; Tao et al. 2003; Huaux et al. 2003; Crystal et al. 2002). Several *in vivo* studies have also demonstrated lung barrier dysfunction and increase in paracellular permeability of the lung endothelium in mice exposed to bleomycin (Yin et al. 2012).

Tight junction proteins of the ECs are responsible for the proper endothelial function (Utech et al. 2006; Van Itallie and Anderson, 2006). These tight junction proteins include zonula occludens-1 (ZO-1) and occludins. The actin-cytoskeleton is another important aspect of the ECs that regulates the endothelial function. The actin microfilaments have been shown to play a critical role in the regulation of the endothelial barrier (Dudek and Garcia, 2001). The ZO-1 and actin-cytoskeleton are linked, and thus any alterations to these proteins greatly affect the endothelial paracellular permeability (Kawkitinarong et al. 2004).

These proteins and their functions are very sensitive to oxidative stress and imbalance in thiol-redox. ROS and 4-hydroxy-2-nonenal (4-HNE) have been shown to play an important role in the disruption in these proteins and the endothelial barrier of the lung microvasculature (Usatyuk et al. 2006; Uchida 2003). Our previous studies have also shown glyoxal, an advanced glycation end product, to cause endothelial barrier dysfunction along with tight junction alterations and actin cytoskeletal rearrangement (Sliman et al. 2010). Other oxidants such as hydrogen peroxide and diamide have been shown to disrupt the ZO-1 and occludin proteins and alter the epithelial barrier function (Chapman et al. 2002; Usatyuk et al. 2003). The results of the current study concurred with these findings revealing that the bleomycin-induced cytoskeletal reorganization, tight junction protein alterations, and barrier dysfunction in ECs were caused by bleomycin through oxidative stress and thiol-redox alterations.

Thiol-protectants such as NAC have been widely studied and found to protect against the oxidant (4-HNE, diamide, hydrogen peroxide)-induced endothelial barrier disruption (Usatyuk et al. 2003). NAC has been studied as a therapeutic drug for pulmonary fibrosis,

but the results have been inconclusive. Studies have also shown NAC to ameliorate the inflammatory and fibrotic response to bleomycin (Serrano-Mollar et al. 2003; Cortijo et al. 2001; Hagiwara et al. 2000). However, the lack of pharmacokinetic data and the ineffectiveness of the NAC therapy in practice necessitate an efficient thiol-therapeutic agent. Moreover, bleomycin has been shown to alter both the intracellular and extracellular thiol-redox state (Iyer et al. 2009). The results of the current study clearly demonstrated that bleomycin caused the loss of GSH and total thiols in ECs, which was restored by the thiol-protectants, NAC and NBMI. Thus, the thiol-redox alterations in the bleomycin-induced lung EC damage and barrier dysfunction seem to be a valid target for therapeutic intervention by effective thiol-protectants.

Overall, the results of the current study clearly demonstrated that the oxidant pulmonary fibrosis inducer, bleomycin, induced cytotoxicity, generation of ROS, loss of thiols, increase in paracellular permeability, cytoskeletal reorganization, and barrier dysfunction in lung ECs, which were all protected by the thiol-protectants suggesting the role of thiol-redox dysregulation in the bleomycin-induced cytotoxicity and barrier dysfunction Scheme 1. Moreover, this study was the first observation to demonstrate that the novel lipid-soluble thiol-protectant, NBMI, was more effective as compared to the commonly used water-soluble thiol-protectant (antioxidant), NAC, in offering protection against the bleomycin-induced cytotoxicity, oxidative stress, thiol-redox dysregulation, and barrier dysfunction. The current study also revealed that NBMI offered remarkable protection against the bleomycin-induced adverse effects at μM dose, whereas mM concentration of NAC was required to achieve such protection in lung ECs.

NBMI structurally resembles the dicarboxybenzoate moiety bound to two cysteamines that is naturally present in fruits. Hence, it is reasonable to expect that NBMI could act as both heavy metal chelator and free radical scavenger. The ability of NBMI to complex with trace heavy metals has been documented (Zaman et al. 2007). The role of iron in the bleomycin-induced oxidative stress has been established and NBMI could also offer protection against the bleomycin-induced EC damage by sequestering iron and rendering it to be inactive in addition to acting as a thiol-protective antioxidant. In addition, the lipophilic nature of NBMI could have been advantageous for the molecule to partition in the lipid-rich hydrophobic microenvironments of the cellular membranes where the redox-regulated biochemical events take place leading to the adverse effects of bleomycin. The emergence of novel bifunctional chelating drugs, such as NBMI, with thiol-redox antioxidant action will offer effective protection against the bleomycin-induced lung vascular damage and also appear as promising therapeutics for IPF in humans.

Acknowledgments

This work was supported by the funds from the Dorothy M. Davis Heart and Lung Research Institute and the Division of Pulmonary, Allergy, Critical Care, and Sleep Medicine of the Ohio State University, the National Institute of Health (HL093463), the International Academy of Oral Medicine and Toxicology (IAOMT), and the Alan D. Clark, M.D. Memorial Research Fund. Boyd E. Haley, a co-author of this communication, is Professor Emeritus in the Department of Chemistry at the University of Kentucky, Lexington, KY, with a 20% research appointment and is on an active NSF grant in that institution. Boyd E. Haley is also President of CTI Science, which is a possible conflict of interest since they hold the license to the patents concerning the compound, NBMI. However, this research project had not been funded or had not been supported or carried out in part or full by CTI Science in any way. Neither Boyd E. Haley nor the CTI Science had any influence or control on this research project. This research project was entirely initiated and supervised by Narasimham L. Parinandi at the Ohio State University, Columbus, OH, with the compound, NBMI synthesized by Niladri Gupta (a graduate student of Boyd E. Haley) in the Department of Chemistry at the University of Kentucky, Lexington, KY, under the supervision of Boyd E. Haley (Professor of Chemistry). Boyd E. Haley is Chair of the Scientific Advisory Committee of the International Academy of Oral Medicine and Toxicology (IAOMT) who advises the IAOMT Board regarding scientific matters when they request it but he does not have any control over IAOMT in their grant funding decision.

making. The IAOMT award has been given exclusively to Narasimham L. Parinandi to conduct research without any influence or control of Boyd E. Haley on this research project.

References

- Antholine WE, Petering DH, Saryan LA, Brown CE. Interactions among iron(II) bleomycin, Lewis bases, and DNA. *Proc Natl Acad Sci USA*. 1981; 78:7517–7520. [PubMed: 6174974]
- Behr J, Ryu JH. Pulmonary hypertension in interstitial lung disease. *Eur Respir J*. 2008; 31:1357–1367. [PubMed: 18515559]
- Bogatcheva NV, Verin AD. The role of cytoskeleton in the regulation of vascular endothelial barrier function. *Microvasc Res*. 2008; 76:202–207. [PubMed: 18657550]
- Burger RM, Peisach J, Blumberg WE, Horwitz SB. Iron-bleomycin interactions with oxygen and oxygen analogues. Effects on spectra and drug activity. *J Biol Chem*. 1979; 254:10906–10912. [PubMed: 91607]
- Calabrese F, Giacometti C, Rea F, Loy M, Valente M. Idiopathic interstitial pneumonias: Primum movens: epithelial, endothelial or whatever. *Sarcoidosis Vasc Diffuse Lung Dis*. 2005; 22(Suppl 1):S15–S23. [PubMed: 16457013]
- Chapman KE, Waters CM, Miller WM. Continuous exposure of airway epithelial cells to hydrogen peroxide: protection by KGF. *J Cell Physiol*. 2002; 192:71–80. [PubMed: 12115738]
- Chiang ET, Camp SM, Dudek SM, Brown ME, Usatyuk PV, Zaborina O, Alverdy JC, Garcia JG. Protective effects of high-molecular weight polyethylene glycol (PEG) in human lung endothelial cell barrier regulation: role of actin cytoskeletal rearrangement. *Microvasc Res*. 2009; 77:174–186. [PubMed: 19121327]
- Cordier JF. Pulmonary hypertension in chronic respiratory and cardiac diseases. *Rev Prat*. 2008; 58:2019–2023. [PubMed: 19143273]
- Cortijo J, Cerda-Nicolas M, Serrano A, Bioque G, Estrela JM, Santangelo F, Esteras A, Llombart-Bosch A, Morcillo EJ. Attenuation by oral N-acetylcysteine of bleomycin-induced lung injury in rats. *Eur Respir J*. 2001; 17:1228–1235. [PubMed: 11491169]
- Crystal RG, Bitterman PB, Mossman B, Schwarz MI, Sheppard D, Almasy L, Chapman HA, Friedman SL, King TE Jr, Leinwand LA, Liotta L, Martin GR, Schwartz DA, Schultz GS, Wagner CR, Musson RA. Future research directions in idiopathic pulmonary fibrosis: summary of a National Heart, Lung, and Blood Institute working group. *Am J Respir Crit Care Med*. 2002; 166:236–246. [PubMed: 12119236]
- Dudek SM, Garcia JG. Cytoskeletal regulation of pulmonary vascular permeability. *J Appl Physiol*. 2001; 91:1487–1500. [PubMed: 11568129]
- Everett RS, Vanhook MK, Barozzi N, Toth I, Johnson LG. Specific modulation of airway epithelial tight junctions by apical application of an occludin peptide. *Mol Pharmacol*. 2006; 69:492–500. [PubMed: 16288084]
- Fang KC. Mesenchymal regulation of alveolar repair in pulmonary fibrosis. *Am J Respir Cell Mol Biol*. 2000; 23:142–145. [PubMed: 10919978]
- Fasano A. Regulation of intercellular tight junctions by zonula occludens toxin and its eukaryotic analogue zonulin. *Ann N Y Acad Sci*. 2000; 915:214–222. [PubMed: 11193578]
- Ghio AJ. Disruption of iron homeostasis and lung disease. *Biochim Biophys Acta*. 2009; 1790:731–739. [PubMed: 19100311]
- Gross TJ, Hunninghake GW. Idiopathic pulmonary fibrosis. *N Engl J Med*. 2001; 345:517–525. [PubMed: 11519507]
- Hagele TJ, Mazerik JN, Gregory A, Kaufman B, Magalang U, Kuppusamy ML, Marsh CB, Kuppusamy P, Parinandi NL. Mercury activates vascular endothelial cell phospholipase D through thiols and oxidative stress. *Int J Toxicol*. 2007; 26:57–69. [PubMed: 17365148]
- Hagiwara SI, Ishii Y, Kitamura S. Aerosolized administration of N-acetylcysteine attenuates lung fibrosis induced by bleomycin in mice. *Am J Respir Crit Care Med*. 2000; 162:225–231. [PubMed: 10903246]
- Harhaj NS, Antonetti DA. Regulation of tight junctions and loss of barrier function in pathophysiology. *Int J Biochem Cell Biol*. 2004; 36:1206–1237. [PubMed: 15109567]

- Huax F, Liu T, McGarry B, Ullenbruch M, Xing Z, Phan SH. Eosinophils and T lymphocytes possess distinct roles in bleomycin-induced lung injury and fibrosis. *J Immunol.* 2003; 171:5470–5481. [PubMed: 14607953]
- Iyer SS, Ramirez AM, Ritzenthaler JD, Torres-Gonzalez E, Roser-Page S, Mora AL, Brigham KL, Jones DP, Roman J, Rojas M. Oxidation of extracellular cysteine/cystine redox state in bleomycin-induced lung fibrosis. *Am J Physiol Lung Cell Mol Physiol.* 2009; 296:L37–L45. [PubMed: 18931052]
- Jackson RM. Pulmonary oxygen toxicity. *Chest.* 1985; 88:900–905. [PubMed: 3905287]
- Kawkitinarong K, Linz-McGillem L, Birukov KG, Garcia JG. Differential regulation of human lung epithelial and endothelial barrier function by thrombin. *Am J Respir Cell Mol Biol.* 2004; 31:517–527. [PubMed: 15284075]
- Kinnula VL, Myllarniemi M. Oxidant-antioxidant imbalance as a potential contributor to the progression of human pulmonary fibrosis. *Antioxid Redox Signal.* 2008; 10:727–738. [PubMed: 18177235]
- Kinnula VL, Fattman CL, Tan RJ, Oury TD. Oxidative stress in pulmonary fibrosis: a possible role for redox modulatory therapy. *Am J Respir Crit Care Med.* 2005; 172:417–422. [PubMed: 15894605]
- Li J, Poovey HG, Rodriguez JF, Brody A, Hoyle GW. Effect of platelet-derived growth factor on the development and persistence of asbestos-induced fibroproliferative lung disease. *J Environ Pathol Toxicol Oncol.* 2004; 23:253–266. [PubMed: 15511213]
- Magro CM, Allen J, Pope-Harman A, Waldman WJ, Moh P, Rothrauff S, Ross P Jr. The role of microvascular injury in the evolution of idiopathic pulmonary fibrosis. *Am J Clin Pathol.* 2003; 119:556–567. [PubMed: 12710128]
- Matlock MM, Howerton BS, Atwood DA. Irreversible precipitation of mercury and lead. *J Hazard Mater.* 2001; 84:73–82. [PubMed: 11376885]
- Matlock, MM.; Howerton, BS.; Atwood, DA. Novel Multidentate Sulfur Containing Ligands. U.S. Patent No. 6,586,600. 2003. July 1, 2003.
- Mazerik JN, Hagele T, Sherwani S, Ciapala V, Butler S, Kuppasamy ML, Hunter M, Kuppasamy P, Marsh CB, Parinandi NL. Phospholipase A2 activation regulates cytotoxicity of methylmercury in vascular endothelial cells. *Int J Toxicol.* 2007; 26:553–569. [PubMed: 18066971]
- Moore BB, Hogaboam CM. Murine models of pulmonary fibrosis. *Am J Physiol Lung Cell Mol Physiol.* 2008; 294:L152–L160. [PubMed: 17993587]
- Oikonomou N, Harokopos V, Zalevsky J, Valavanis C, Kotanidou A, Szymkowski DE, Kollias G, Aidinis V. Soluble TNF mediates the transition from pulmonary inflammation to fibrosis. *PLoS ONE.* 2006; 1:e108. [PubMed: 17205112]
- Parinandi NL, Scribner WM, Vepa S, Shi S, Natarajan V. Phospholipase D activation in endothelial cells is redox sensitive. *Antioxid Redox Signal.* 1999; 1:193–210. [PubMed: 11228747]
- Parinandi NL, Roy S, Shi S, Cummings RJ, Morris AJ, Garcia JG, Natarajan V. Role of Src kinase in diperoxovanadate-mediated activation of phospholipase D in endothelial cells. *Arch Biochem Biophys.* 2001; 396:231–243. [PubMed: 11747302]
- Patel RB, Kotha SR, Sherwani SI, Sliman SM, Gurney TO, Loar B, Butler SO, Morris AJ, Marsh CB, Parinandi NL. Pulmonary fibrosis inducer, bleomycin, causes redox-sensitive activation of phospholipase D and cytotoxicity through formation of bioactive lipid signal mediator, phosphatidic acid, in lung microvascular endothelial cells. *Int J Toxicol.* 2011; 30:69–90. [PubMed: 21131602]
- Petri B, Bixel MG. Molecular events during leukocyte diapedesis. *FEBS J.* 2006; 273:4399–4407. [PubMed: 16965541]
- Rojas M, Xu J, Woods CR, Mora AL, Spears W, Roman J, Brigham KL. Bone marrow-derived mesenchymal stem cells in repair of the injured lung. *Am J Respir Cell Mol Biol.* 2005; 33:145–152. [PubMed: 15891110]
- Ryu JH, Krowka MJ, Pellikka PA, Swanson KL, McGoan MD. Pulmonary hypertension in patients with interstitial lung diseases. *Mayo Clin Proc.* 2007; 82:342–350. [PubMed: 17352370]
- Serrano-Mollar A, Closa D, Prats N, Blesa S, Martinez-Losa M, Cortijo J, Estrela JM, Morcillo EJ, Bulbena O. *In vivo* antioxidant treatment protects against bleomycin-induced lung damage in rats. *Br J Pharmacol.* 2003; 138:1037–1048. [PubMed: 12684259]

- Sliman SM, Eubank TD, Kotha SR, Kuppusamy ML, Sherwani SI, Butler ES, Kuppusamy P, Roy S, Marsh CB, Stern DM, Parinandi NL. Hyperglycemic oxoaldehyde, glyoxal, causes barrier dysfunction, cytoskeletal alterations, and inhibition of angiogenesis in vascular endothelial cells: aminoguanidine protection. *Mol Cell Biochem.* 2010; 333:9–26. [PubMed: 19585224]
- Steinhour E, Sherwani SI, Mazerik JN, Ciapala V, O'Connor Butler E, Cruff JP, Magalang U, Parthasarathy S, Sen CK, Marsh CB, Kuppusamy P, Parinandi NL. Redox-active antioxidant modulation of lipid signaling in vascular endothelial cells: vitamin C induces activation of phospholipase D through phospholipase A2, lipoxygenase, and cyclooxygenase. *Mol Cell Biochem.* 2008; 315:97–112. [PubMed: 18496733]
- Tao F, Gonzalez-Flecha B, Kobzik L. Reactive oxygen species in pulmonary inflammation by ambient particulates. *Free Radic Biol Med.* 2003; 35:327–340. [PubMed: 12899936]
- Tashiro M, Izumikawa K, Yoshioka D, Nakamura S, Kurihara S, Sakamoto N, Seki M, Kakeya H, Yamamoto Y, Yanagihara K, Mukae H, Hayashi T, Fukushima K, Tashiro T, Kohno S. Lung fibrosis 10 years after cessation of bleomycin therapy. *Tohoku J Exp Med.* 2008; 216:77–80. [PubMed: 18719341]
- Taskar V, Coultas D. Exposures and idiopathic lung disease. *Semin Respir Crit Care Med.* 2008; 29:670–679. [PubMed: 19221965]
- Uchida K. 4-Hydroxy-2-nonenal: a product and mediator of oxidative stress. *Prog Lipid Res.* 2003; 42:318–343. [PubMed: 12689622]
- Usatyuk PV, Parinandi NL, Natarajan V. Redox regulation of 4-hydroxy-2-nonenal-mediated endothelial barrier dysfunction by focal adhesion, adherens, and tight junction proteins. *J Biol Chem.* 2006; 281:35554–35566. [PubMed: 16982627]
- Usatyuk PV, Vepa S, Watkins T, He D, Parinandi NL, Natarajan V. Redox regulation of reactive oxygen species-induced p38 MAP kinase activation and barrier dysfunction in lung microvascular endothelial cells. *Antioxid Redox Signal.* 2003; 5:723–730. [PubMed: 14588145]
- Utech M, Bruwer M, Nusrat A. Tight junctions and cell-cell interactions. *Methods Mol Biol.* 2006; 341:185–195. [PubMed: 16799199]
- Vaillant P, Menard O, Vignaud JM, Martinet N, Martinet Y. The role of cytokines in human lung fibrosis. *Monaldi Arch Chest Dis.* 1996; 51:145–152. [PubMed: 8680382]
- Van Itallie CM, Anderson JM. Claudins and epithelial paracellular transport. *Annu Rev Physiol.* 2006; 68:403–429. [PubMed: 16460278]
- Vandenbroucke E, Mehta D, Minshall R, Malik AB. Regulation of endothelial junctional permeability. *Ann N Y Acad Sci.* 2008; 1123:134–145. [PubMed: 18375586]
- Varadharaj S, Steinhour E, Hunter MG, Watkins T, Baran CP, Magalang U, Kuppusamy P, Zweier JL, Marsh CB, Natarajan V, Parinandi NL. Vitamin C-induced activation of phospholipase D in lung microvascular endothelial cells: regulation by MAP kinases. *Cell Signal.* 2006; 18:1396–1407. [PubMed: 16376521]
- Warshamana GS, Pociask DA, Fisher KJ, Liu JY, Sime PJ, Brody AR. Titration of non-replicating adenovirus as a vector for transducing active TGF-beta1 gene expression causing inflammation and fibrogenesis in the lungs of C57BL/6 mice. *Int J Exp Pathol.* 2002; 83:183–201. [PubMed: 12485463]
- Wilson MS, Wynn TA. Pulmonary fibrosis: pathogenesis, etiology and regulation. *Mucosal Immunol.* 2009; 2:103–121. [PubMed: 19129758]
- Xu Y, Gong B, Yang Y, Awasthi YC, Woods M, Boor PJ. Glutathione-S-transferase protects against oxidative injury of endothelial cell tight junctions. *Endothelium.* 2007; 14:333–343. [PubMed: 18080870]
- Yin Q, Nan H, Yan L, Huang X, Wang W, Cui G, Wei J. Alteration of tight junctions in pulmonary microvascular endothelial cells in bleomycin-treated rats. *Exp Toxicol Pathol.* 2012; 64:81–91. [PubMed: 20663652]
- Zaman KM, Blue LY, Huggins FE, Atwood DA. Cd, Hg, Pb Compounds of Benzene-1,3-diamidoethanethiol (BDETH(2)). *Inorg Chem.* 2007; 46:1975–1980. [PubMed: 17323915]
- Zisman DA, Keane MP, Belperio JA, Strieter RM, Lynch JP 3rd. Pulmonary fibrosis. *Methods Mol Med.* 2005; 117:3–44. [PubMed: 16130230]

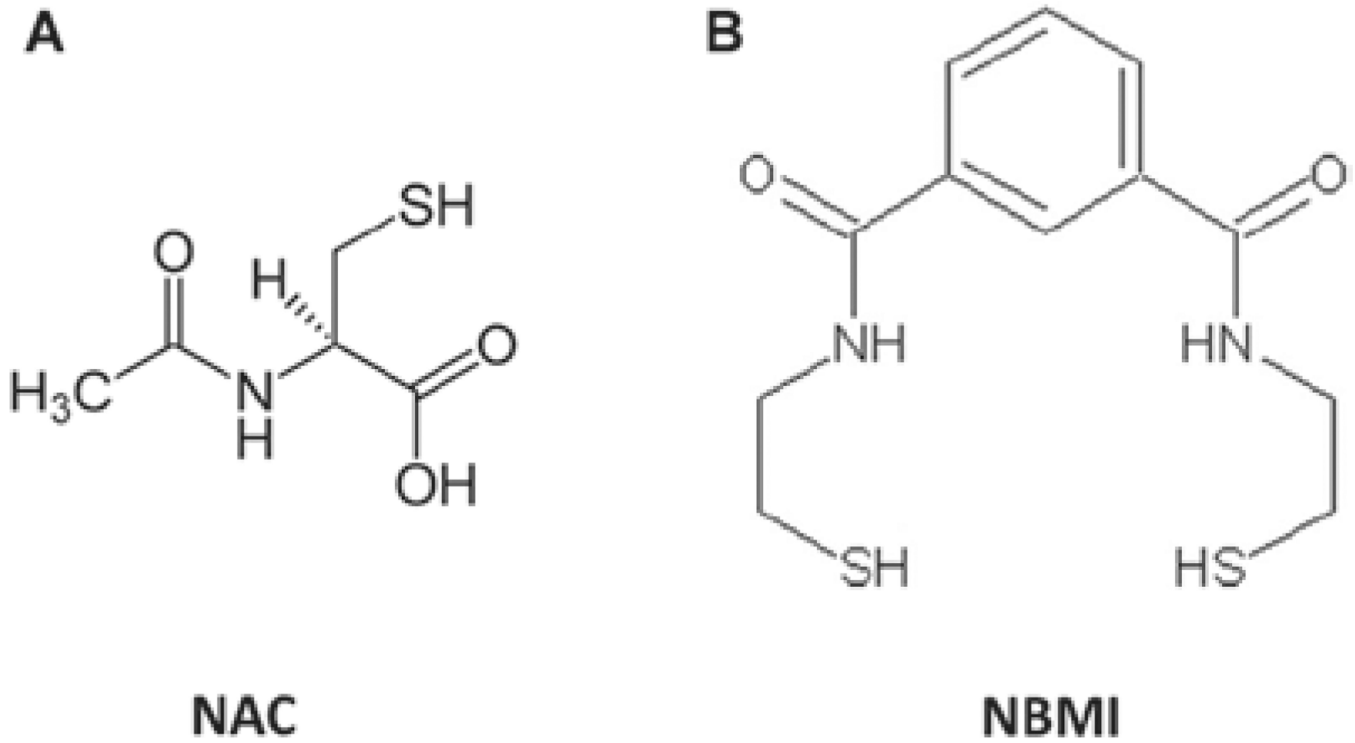


Figure 1. Chemical structure of antioxidants: *N*-acetyl-L-cysteine (NAC) [A] and *N,N'*-bis-2-mercaptoethyl isophthalamide (NBMI) [B].

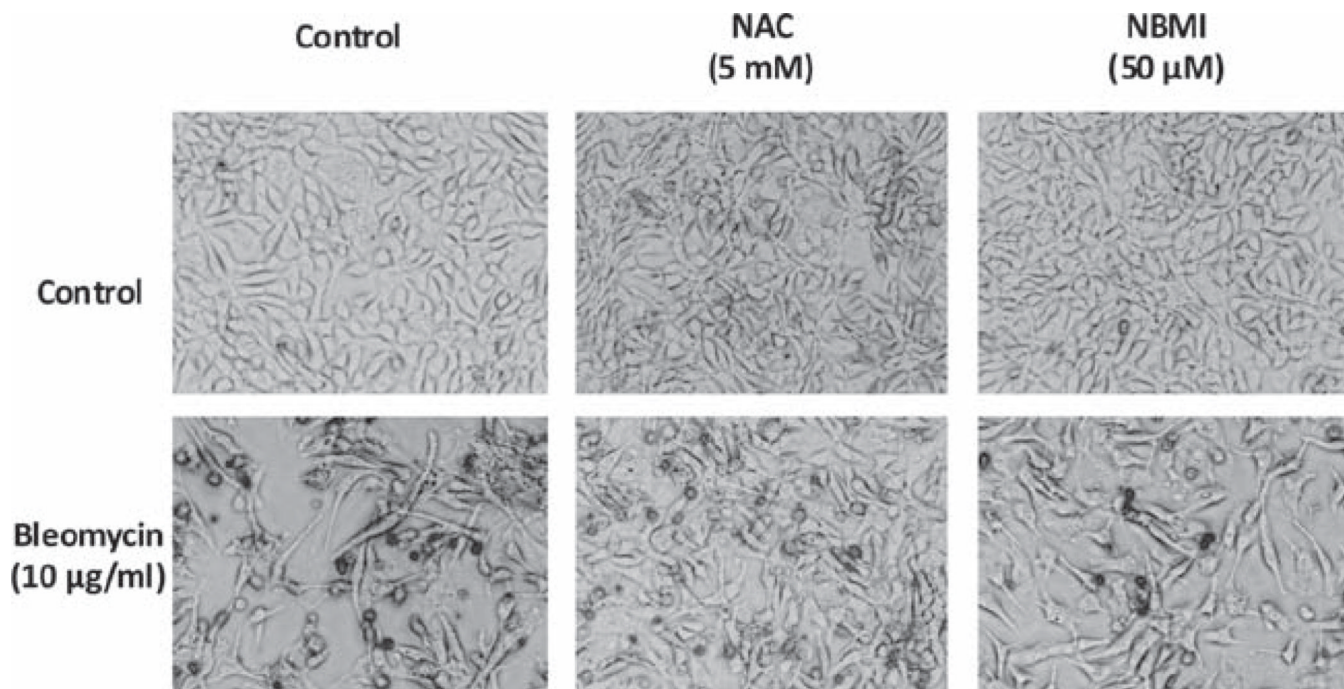


Figure 2. NAC and NBMI protect against bleomycin-induced morphological alterations in ECs. BPAECs (5×10^5 cells/35-mm dish) were pretreated with MEM or MEM containing the chosen antioxidant (5 mM NAC and 50 μ M NBMI) for 1 h and then subjected to co-treatment with MEM containing bleomycin (10 μ g) for 12 h to determine the protective effect of the antioxidants on bleomycin-induced cell morphology alterations. At the end of the incubation period, the cell morphology was examined under light microscope (as an index of EC monolayer disruption and cytotoxicity) as described under the section “Materials and Methods”. Each micrograph is a representative picture obtained from three independent experiments conducted under identical conditions.

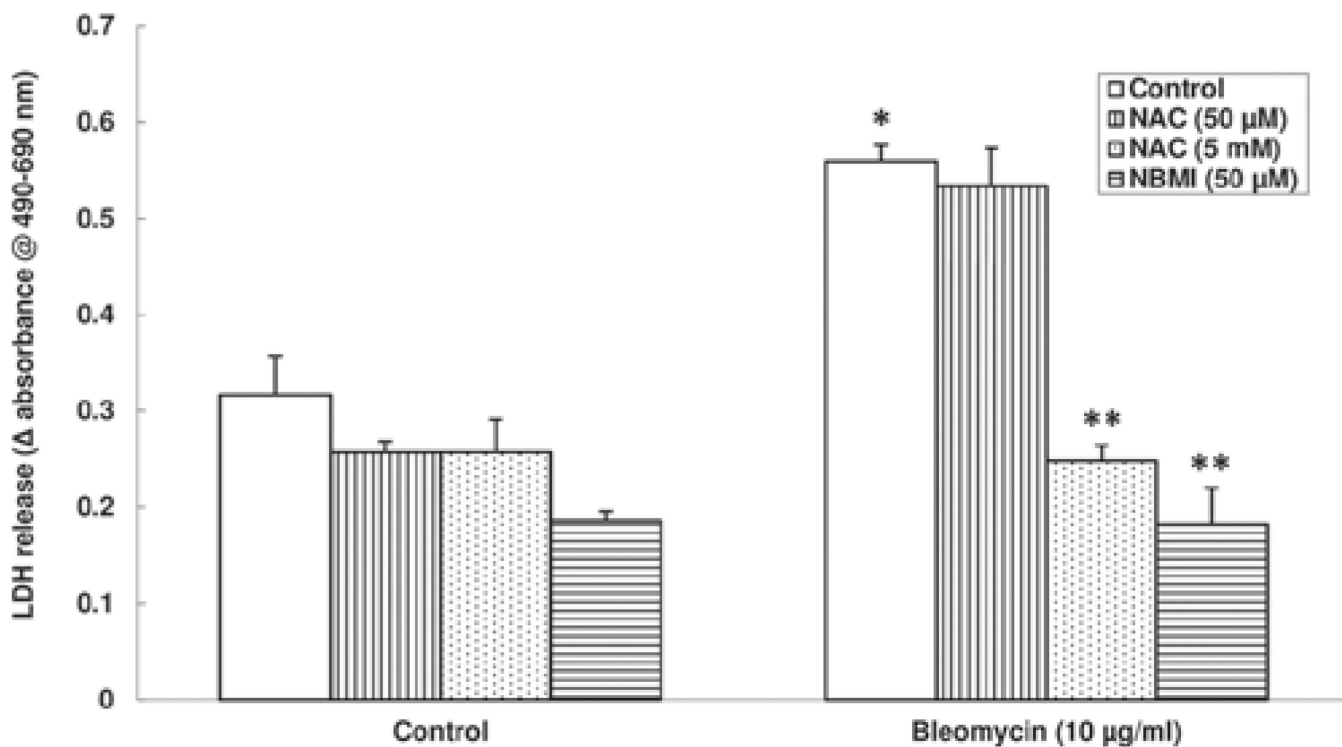


Figure 3.

NAC and NBMI protect against bleomycin-induced cytotoxicity in ECs. BPAECs (2.5×10^5 cells/17.5-mm dish) were pre-treated with MEM alone or MEM containing the chosen antioxidant (50 μM and 5 mM NAC and 50 μM NBMI) for 1 h and then subjected to co-treatment with MEM containing bleomycin (10 μg) for 6 h. At the end of the incubation period, release of LDH into the medium (as an index of cytotoxicity) was determined spectrophotometrically as described under Materials and Methods. Data represent mean \pm SD calculated from three independent experiments. *Significantly different at $p < 0.05$ as compared to cells treated with MEM alone. **Significantly different at $p < 0.05$ as compared to cells treated with MEM containing bleomycin alone.

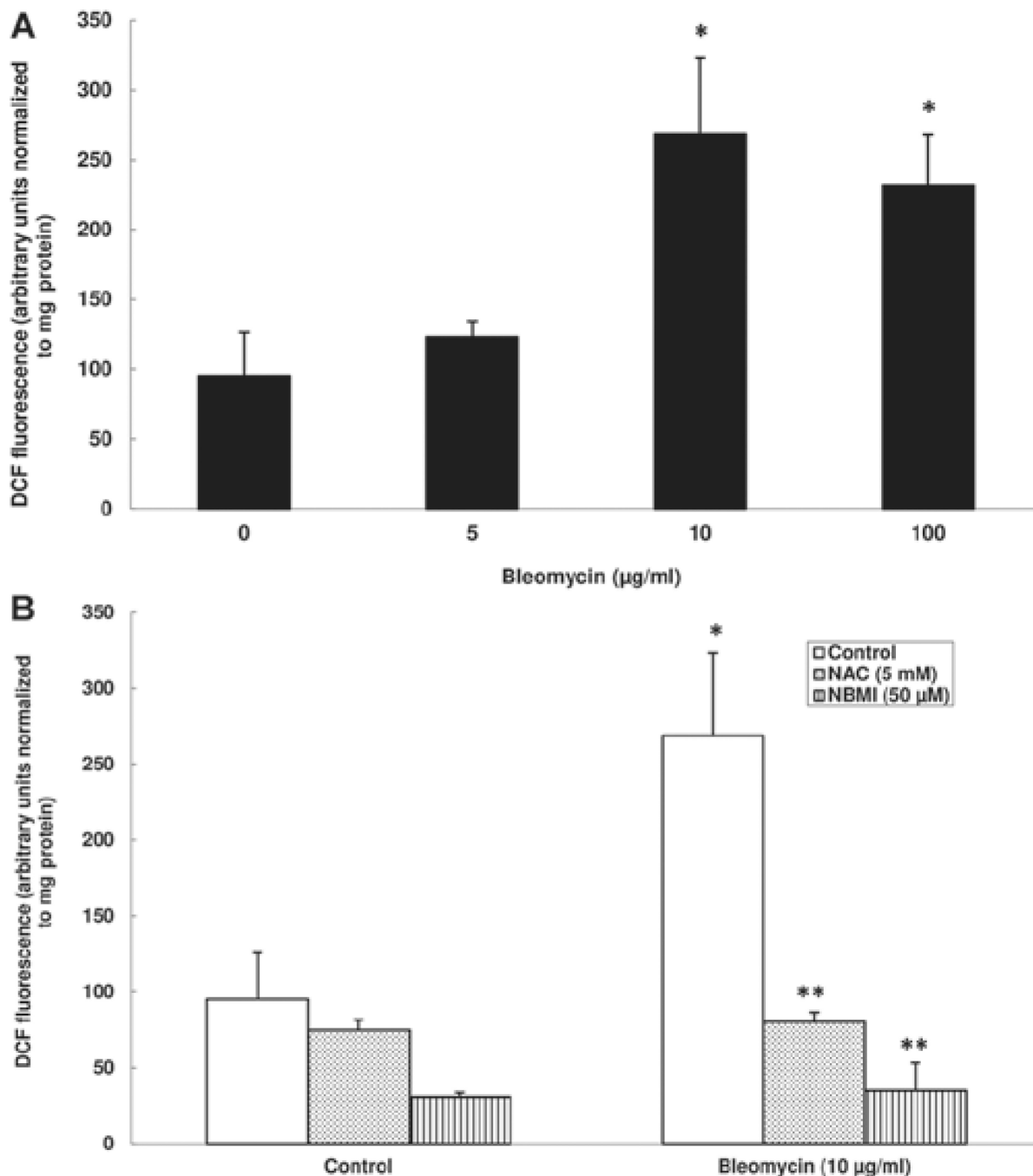
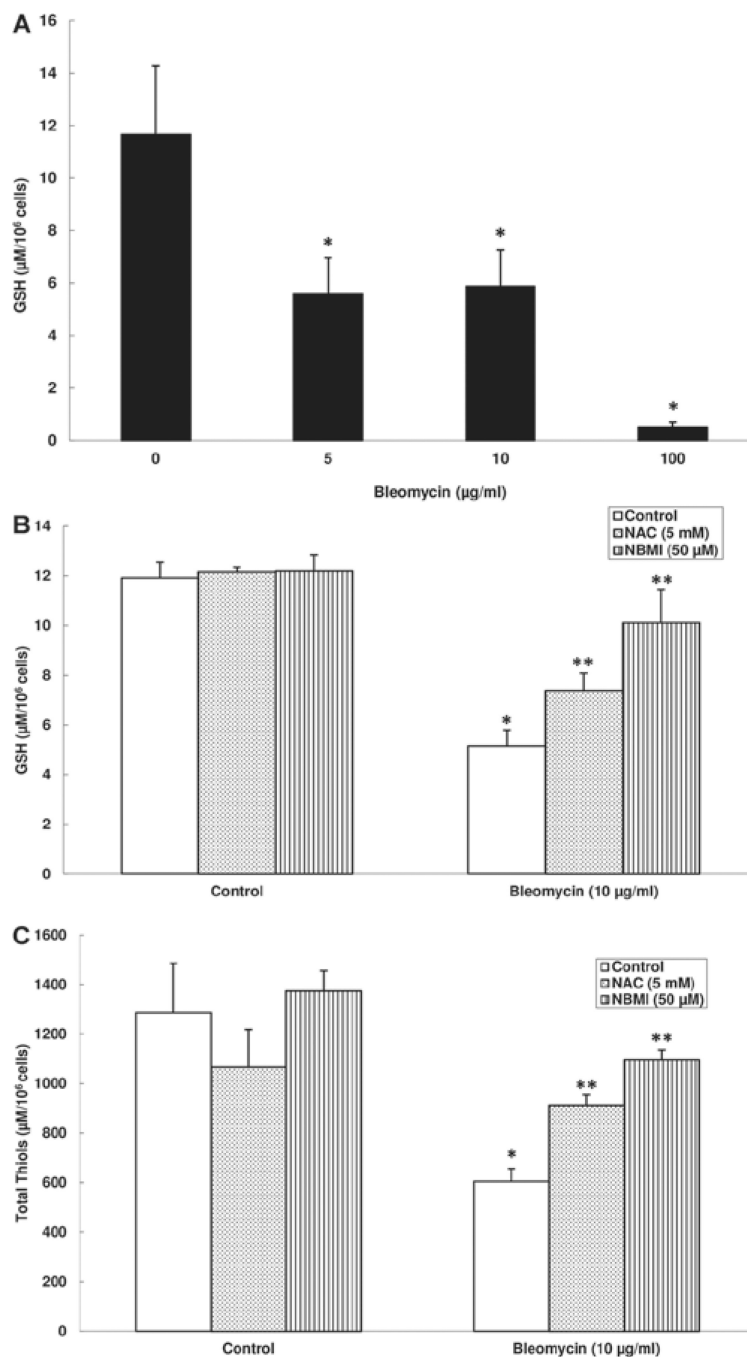


Figure 4.

NAC and NBMI protect against bleomycin-induced ROS generation in ECs. BPAECs (5×10^5 cells/35-mm dish) were preloaded with $10 \mu\text{M}$ DCFDA for 30 min in complete MEM to determine ROS generation. Following the DCFDA loading, cells were subjected to treatment with MEM alone or MEM containing bleomycin (5, 10, and $100 \mu\text{g}$) for 1 h (A). BPAECs were also pretreated with MEM or MEM containing the chosen antioxidant (5 mM NAC and $50 \mu\text{M}$ NBMI) for 1 h and then subjected to co-treatment with MEM containing bleomycin ($10 \mu\text{g}$) for 1 h (B). At the end of the incubation period, the DCF fluorescence (as an index of ROS formation) was determined as described under Materials and Methods.

Data represent mean \pm SD calculated from three independent experiments. *Significantly different at $p < 0.05$ as compared to cells treated with MEM alone. **Significantly different at $p < 0.05$ as compared to cells treated with MEM containing bleomycin alone.

**Figure 5.**

NAC and NBMI protect against bleomycin-induced GSH and total thiols depletion in ECs. BPAECs (1×10^5 cells/96 well plates) were subjected to treatment with MEM alone or MEM containing bleomycin (5, 10, and 100 μg) for 12 h to determine intracellular GSH levels (A). BPAECs were also pre-treated with MEM or MEM containing the chosen antioxidant (5 mM NAC and 50 μM NBMI) for 1 h and then subjected to co-treatment with MEM containing bleomycin (10 μg) for 12 h (B). At the end of the incubation period, the intracellular soluble thiol (GSH) concentrations were determined as described under Materials and Methods. BPAECs (5×10^5 cells/35-mm dish) were pre-treated with MEM or

MEM containing the chosen antioxidant (5 mM NAC and 50 μ M NBMI) for 1 h and then subjected to co-treatment with MEM containing bleomycin (10 μ g) for 12 h (C). At the end of the incubation period, the total thiol concentrations were determined as described under Materials and Methods. Data represent mean \pm SD calculated from three independent experiments. *Significantly different at $p < 0.05$ as compared to cells treated with MEM alone. **Significantly different at $p < 0.05$ as compared to cells treated with MEM containing bleomycin alone.

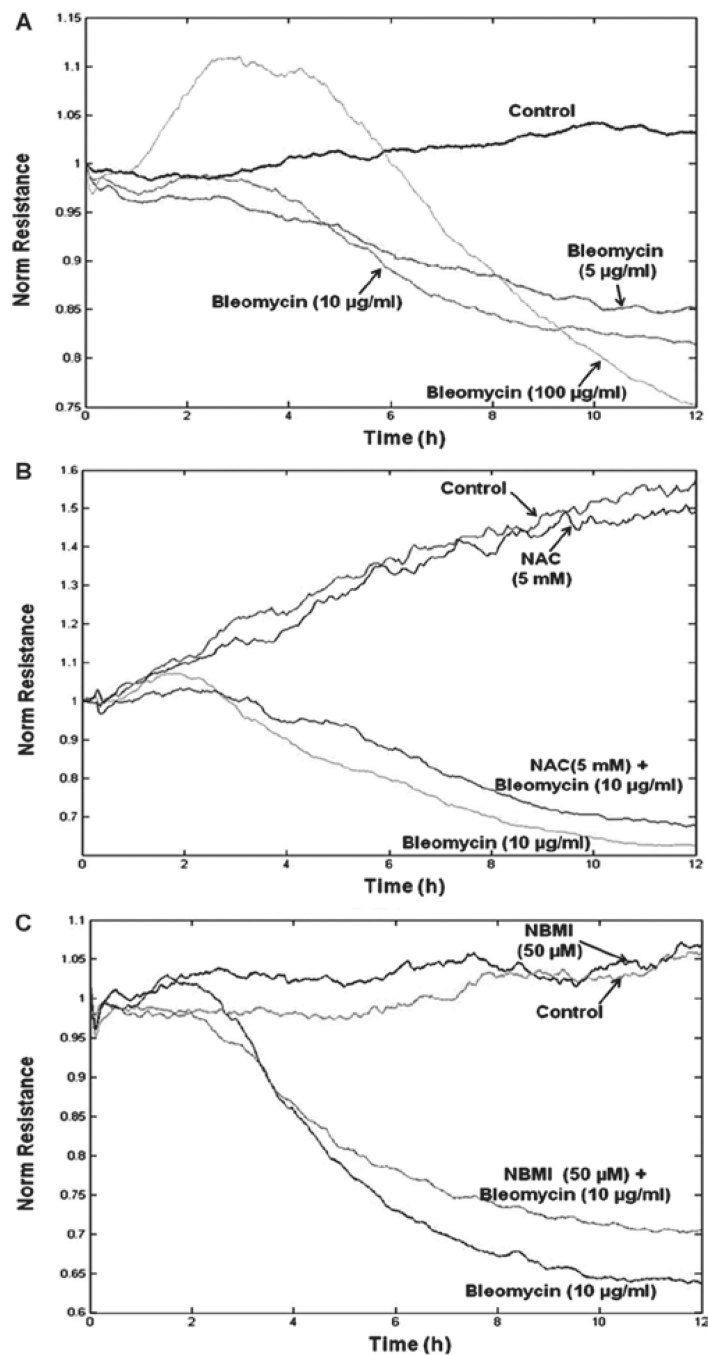


Figure 6. NAC and NBMI protect against bleomycin-induced transendothelial barrier dysfunction. BPAECs grown on gold electrodes were subjected to treatment with MEM alone or MEM containing bleomycin (5, 10, and 100 μg) (A). BPAECs were also pre-treated with MEM or MEM containing 5 mM NAC (B) or 50 μM NBMI (C) for 1 h and then subjected to co-treatment with MEM containing bleomycin (10 μg). The transendothelial electrical resistance was measured continuously in an ECIS system as described under Materials and Methods.

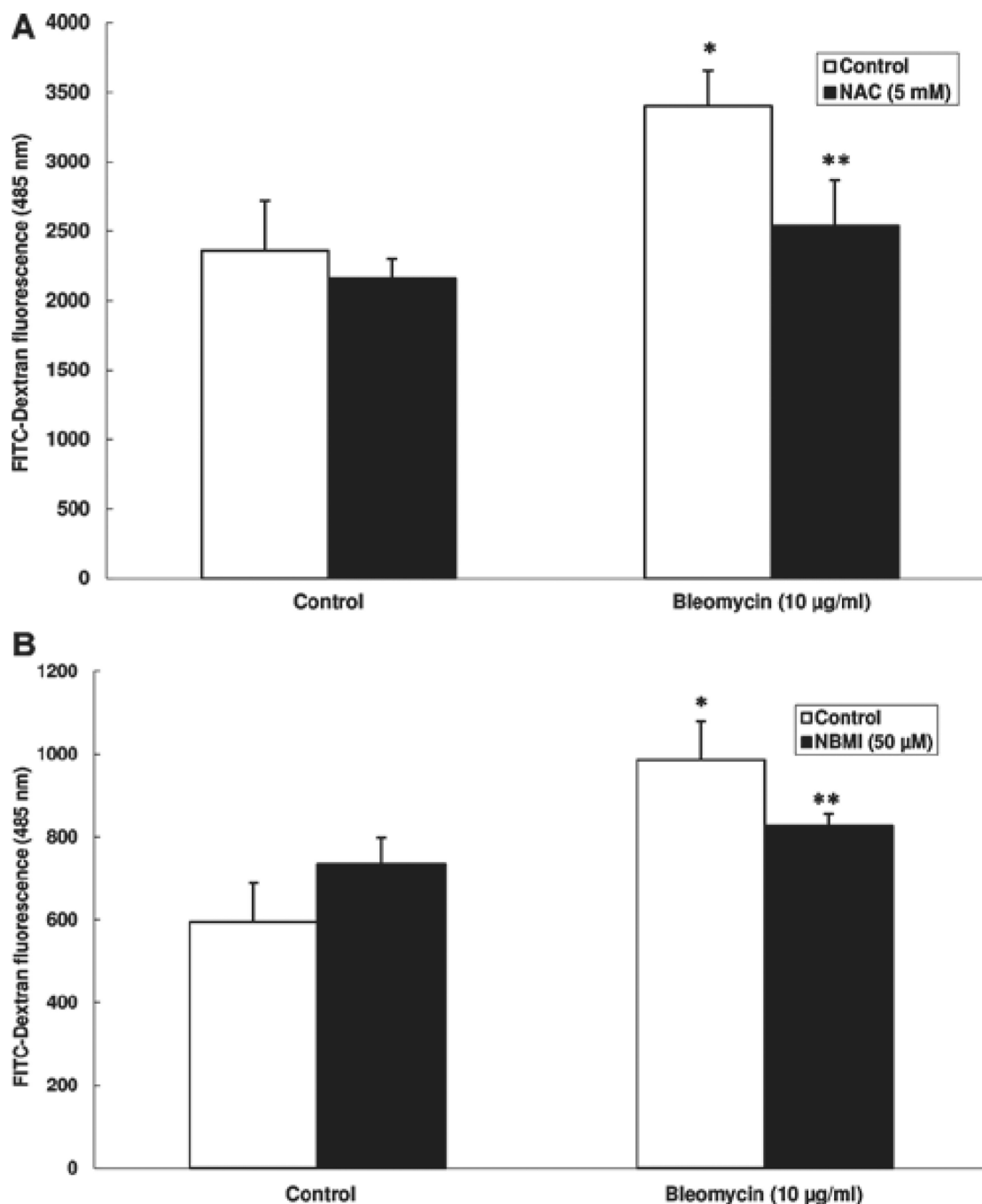


Figure 7.

NAC and NBMI protect against bleomycin-induced paracellular permeability in the EC monolayer. BPAECs grown on 3.0 µm pore-size culture inserts were subjected to treatment with MEM alone or MEM containing 5 mM NAC (A) or 50 µM NBMI (B) for 1 h and then subjected to co-treatment with MEM containing bleomycin (10 µg) for 12 h. The paracellular leak in the EC monolayer was measured as described under Materials and Methods. Data represent mean ± SD calculated from three independent experiments.

*Significantly different at $p < 0.05$ as compared to cells treated with MEM alone.

**Significantly different at $p < 0.05$ as compared to cells treated with MEM containing bleomycin alone.

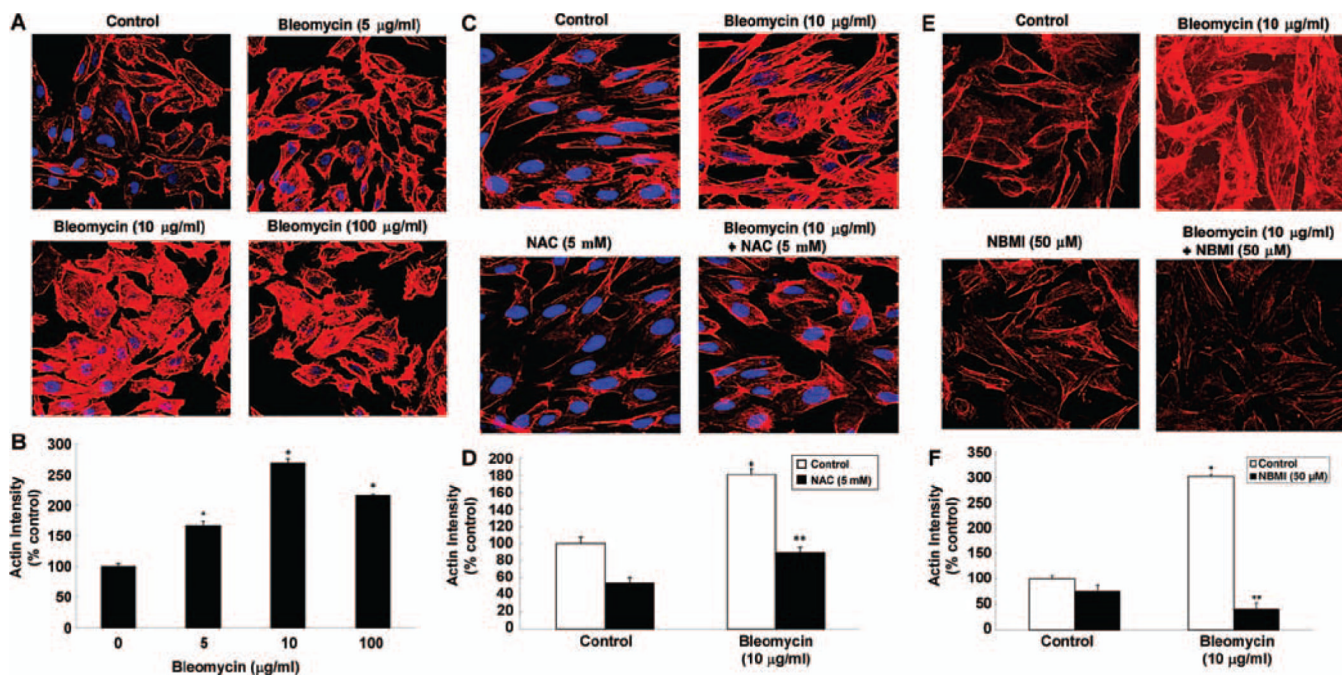


Figure 8.

NAC and NBMI protect against bleomycin-induced actin cytoskeletal reorganization in ECs. BPAECs on coverslips (5×10^5 cells/35-mm dish) were subjected to treatment with MEM alone or MEM containing bleomycin (5, 10, and 100 µg) for 4 h (A,B). BPAECs were also pre-treated with MEM or MEM containing 5 mM NAC (C,D) or 50 µM NBMI (E,F) for 1 h and then subjected to co-treatment with MEM containing bleomycin (10 µg) for 4 h to assay the extent of actin cytoskeletal reorganization. At the end of the incubation period, the cells were fixed and stained as described under Materials and Methods. The fluorescence intensities were measured as described under Materials and Methods. Each micrograph is a representative picture obtained from three independent experiments conducted under identical conditions. Data represent mean \pm SD calculated from three independent experiments. *Significantly different at $p < 0.05$ as compared to cells treated with MEM alone. **Significantly different at $p < 0.05$ as compared to cells treated with MEM containing bleomycin alone.

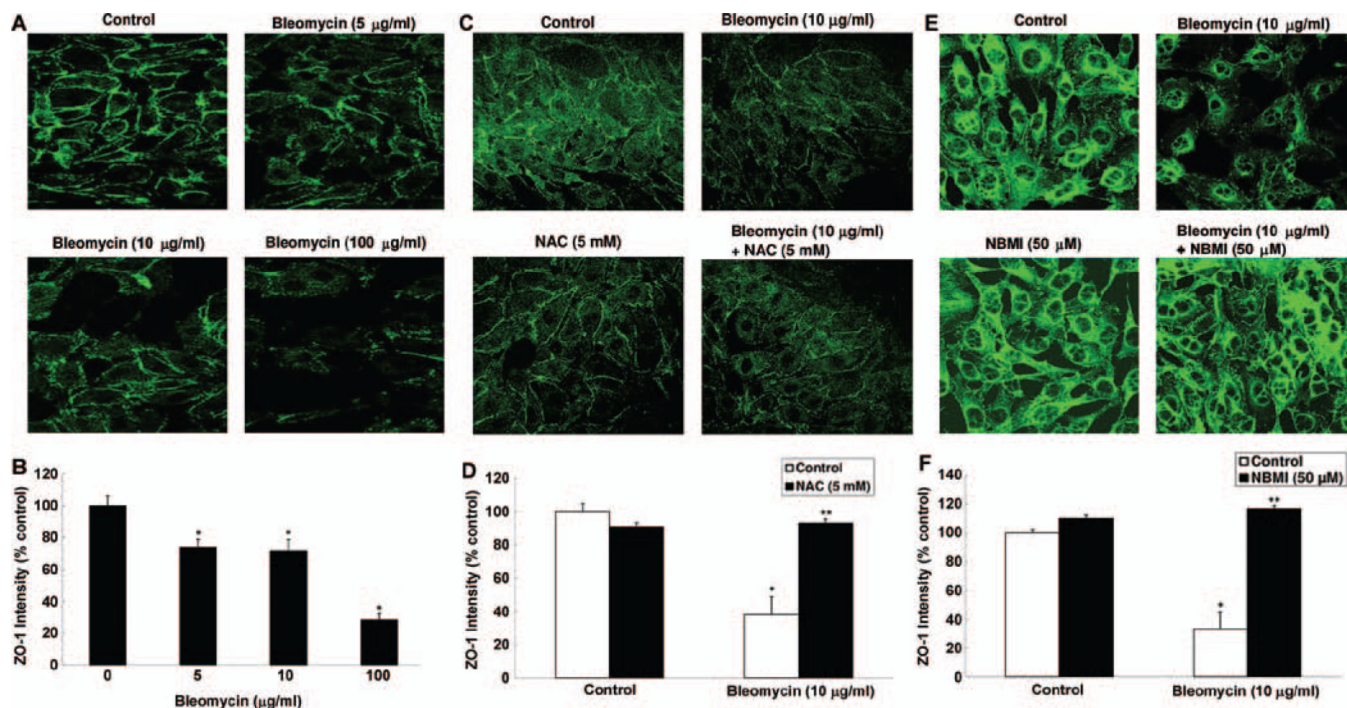


Figure 9.

NAC and NBMI protect against bleomycin-induced tight junction protein, ZO-1, alterations in ECs. BPAECs on coverslips (5×10^5 cells/35-mm dish) were subjected to treatment with MEM alone or MEM containing bleomycin (5, 10, and 100 μg) for 4 h (A,B). BPAECs were also pre-treated with MEM or MEM containing 5 mM NAC (C,D) or 50 μM NBMI (E,F) for 1 h and then subjected to co-treatment with MEM containing bleomycin (10 μg) for 4 h. At the end of the incubation period, the cells were fixed and stained as described under Materials and Methods. The fluorescence intensities were measured as described under Materials and Methods. Each micrograph is a representative picture obtained from three independent experiments conducted under identical conditions. Data represent mean \pm SD calculated from three independent experiments. *Significantly different at $p < 0.05$ as compared to cells treated with MEM alone. **Significantly different at $p < 0.05$ as compared to cells treated with MEM containing bleomycin alone.

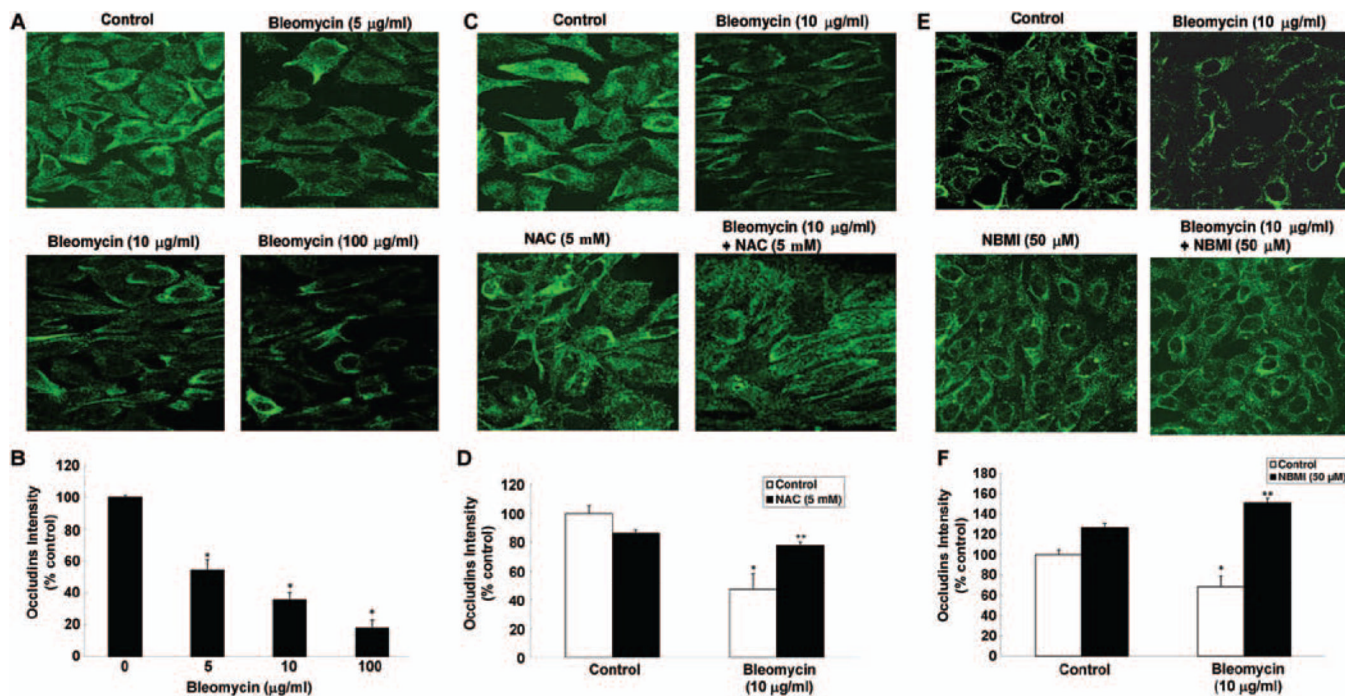


Figure 10.

NAC and NBMI protect against the bleomycin-induced tight junction protein, occludin, alterations in ECs. BPAECs on coverslips (5×10^5 cells/35-mm dish) were subjected to treatment with MEM alone or MEM containing bleomycin (5, 10, and 100 µg) for 4 h (A,B). BPAECs were also pre-treated with MEM or MEM containing 5 mM NAC (C,D) or 50 µM NBMI (E,F) for 1 h and then subjected to co-treatment with MEM containing bleomycin (10 µg) for 4 h. At the end of the incubation period, the cells were fixed and stained as described under Materials and Methods. The fluorescence intensities were measured as described under Materials and Methods. Each micrograph is a representative picture obtained from three independent experiments conducted under identical conditions. Data represent mean \pm SD calculated from three independent experiments. *Significantly different at $p < 0.05$ as compared to cells treated with MEM alone. **Significantly different at $p < 0.05$ as compared to cells treated with MEM containing bleomycin alone.

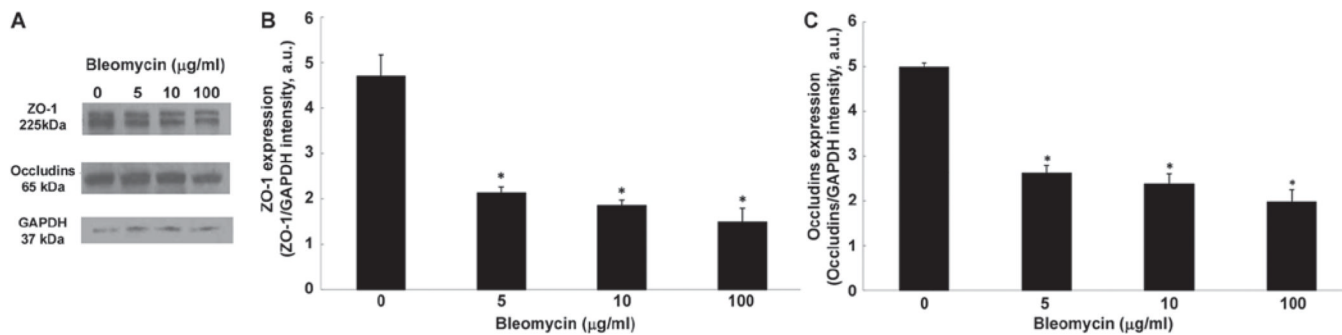
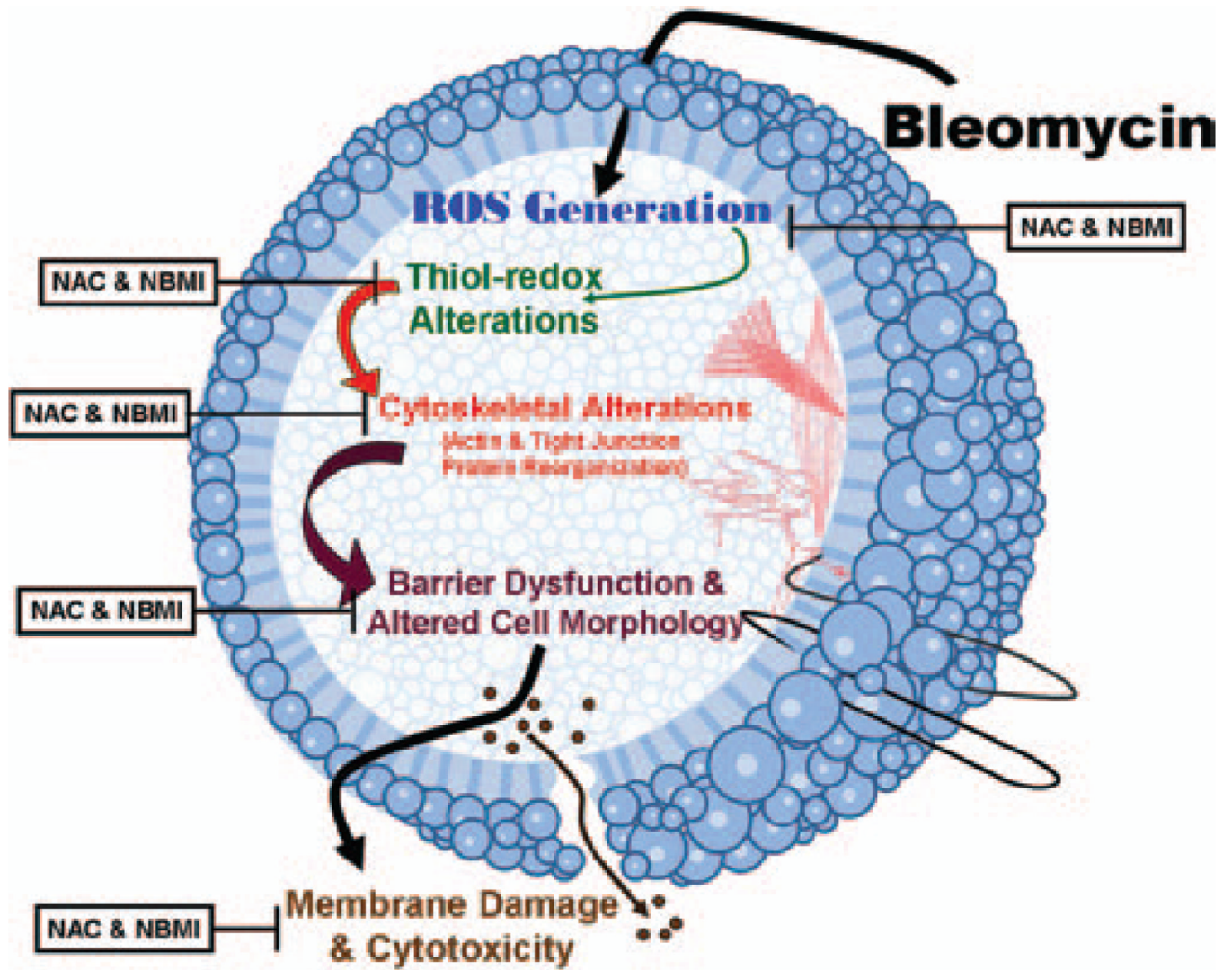


Figure 11.

Bleomycin causes loss of tight junction proteins in ECs. BPAECs (5×10^5 cells/35-mm dish) were subjected to treatment with MEM alone or MEM containing bleomycin (5, 10, and 100 µg) for 4 h (A). At the end of the incubation period, the expression of the tight junction protein was determined using Western blotting as described under Materials and Methods. The blot intensities of the protein expression, normalized to the GAPDH expression intensity, were determined using the Scion Imaging software. Data represent mean \pm SD calculated from three independent experiments. *Significantly different at $p < 0.05$ as compared to cells treated with MEM alone.



Scheme 1.
Proposed mechanism. Schematic representation of bleomycin-induced thiol alterations, cytotoxicity, and the subsequent endothelial barrier dysfunction and damage.